

# AMP-Activated Protein Kinase Activation by AICAR Increases Both Muscle Fatty Acid and Glucose Uptake in White Muscle of Insulin-Resistant Rats In Vivo

Miguel A. Iglesias, Stuart M. Furler, Gregory J. Cooney, Edward W. Kraegen, and Ji-Ming Ye

**Insulin-stimulated glucose uptake is increased in white but not red muscle of insulin-resistant high-fat-fed (HF) rats after administration of the AMP-activated protein kinase (AMPK) activator 5-aminoimidazole-4-carboxamide-1- $\beta$ -D-ribofuranoside (AICAR). To investigate whether a lesser AICAR effect on glucose uptake in red muscle was offset by a greater effect on fatty acid (FA) uptake, we examined acute effects of AICAR on muscle glucose and FA fluxes in HF rats. HF rats received AICAR (250 mg/kg) subcutaneously. At 30 min, a mixture of either  $^3\text{H}$ -(R)-2-bromopalmitate/ $^{14}\text{C}$ -palmitate or  $^3\text{H}$ -2-deoxyglucose/ $^{14}\text{C}$ -glucose was administered intravenously to assess muscle FA and glucose uptake. AICAR decreased plasma levels of glucose (~25%), insulin (~60%), and FAs (~30%) at various times over the next 46 min ( $P < 0.05$  vs. controls). In white muscle, AICAR increased both FA (2.4-fold) and glucose uptake (4.9-fold), associated with increased glycogen synthesis (6-fold). These effects were not observed in red muscle. We conclude that both glucose and FA fluxes are enhanced by AICAR more in white versus red muscle, consistent with the relative degree of activation of AMPK. Therefore, a lesser effect of AICAR to alleviate muscle insulin resistance in red versus white muscle is not explained by a relatively greater effect on FA uptake in the red muscle. *Diabetes* 53:1649–1654, 2004**

**R**ecent evidence suggests that AMP-activated protein kinase (AMPK) is involved in mediating metabolic responses of muscle to exercise (1,2). During muscle contraction, AMPK is activated by an elevation in the AMP-to-ATP ratio as a result of ATP depletion (3). Activated AMPK inhibits acetyl-CoA carboxylase and stimulates malonyl-CoA decarboxylase (4), thus decreasing malonyl-CoA content. Reduction in malonyl-CoA diminishes the inhibition of carnitine palmitoyltransferase-1, allowing fatty acid (FA) entry into mitochondria for oxidation. In addition, AMPK mediates an increase in

glucose uptake by stimulating GLUT4 translocation to the plasma membrane (5).

AMPK can also be activated pharmacologically by the AMP analog 5-aminoimidazole-4-carboxamide-1- $\beta$ -D-ribofuranoside (AICAR) independent of changes in the AMP-to-ATP ratio (6). This offers a useful tool to investigate AMPK-mediated metabolic changes in vivo, particularly in muscle, where its action on hexose transport is specific to AMPK activation (7). We have recently shown that administration of AICAR to insulin-resistant high-fat-fed (HF) rats results in an enhancement of insulin-stimulated glucose uptake in muscle 24 h later (8). This enhanced insulin action was more apparent in white than in red muscle. AICAR-related effects on muscle glucose uptake were present after acute AICAR-stimulated AMPK activity had declined, and we postulated that effects may be due in part to different muscle type-specific effects of AICAR to regulate glucose and lipid metabolism in this model. AICAR has been reported to preferentially increase glucose uptake in white versus red muscle (9), although the relative effects on fatty acid uptake are not known. If AICAR had a relatively greater effect to enhance FA uptake in red muscle, then it might partly offset a lesser effect on glucose uptake in this tissue. In addition, if enhanced FA uptake increased cytosolic lipid accumulation, a factor associated with insulin resistance (10), then it would help to explain subsequent differential effects on insulin sensitivity in red versus white muscle in our insulin-resistant model. Therefore, the aim of the present study was to investigate the acute effects of AICAR on lipid and glucose metabolism in muscle of HF rats and possible links to enhanced insulin action as demonstrated previously (8). The study used [9,10- $^3\text{H}$ ](R)-2-bromopalmitate ( $^3\text{H}$ -R-BrP) tracer in combination with  $^{14}\text{C}$ -palmitate to determine the uptake and fate of FAs. In separate experiments, a combination of 2-deoxy-D-(2,6- $^3\text{H}$ )-glucose (2DG) and  $^{14}\text{C}$ -glucose was used to assess the effects on glucose metabolism in muscle under the same conditions.

## RESEARCH DESIGN AND METHODS

Male Wistar rats (~300 g) purchased from the Animal Resources Centre (Perth, Australia) were used for the study. All experimental procedures were approved by the Animal Experimentation Ethics Committee (Garvan Institute/St. Vincent's Hospital) and were in accordance with the National Health and Medical Research Council of Australia Guidelines on Animal Experimentation. The animals were housed at  $22 \pm 0.5^\circ\text{C}$  with a 12/12-h day/night cycle (lights on at 0600) and fed a standard diet (Rat maintenance diet; Gordons Specialty Feeds, Sydney, Australia) ad libitum for 1 week. After this acclimatization, they were fed an isocaloric high-fat diet (350 kJ/day given at 1600) for 3 weeks. The nutrient composition of the fat diet expressed as a percentage of

From the Garvan Institute of Medical Research, Sydney, Australia.

Address correspondence and reprint requests to Edward W. Kraegen, PhD, Diabetes and Obesity Program, Garvan Institute of Medical Research, 384 Victoria St., Darlinghurst, NSW 2010, Australia. E-mail: e.kraegen@garvan.org.au.

Received for publication 26 September 2003 and accepted in revised form 29 March 2004.

2DG, 2-deoxy-D-(2,6- $^3\text{H}$ )-glucose;  $^3\text{H}$ -R-BrP, [9,10- $^3\text{H}$ ](R)-2-bromopalmitate; ACS, acyl-CoA synthetase; AICAR, 5-aminoimidazole-4-carboxamide-1- $\beta$ -D-ribofuranoside; AMPK, AMP-activated protein kinase; FA, fatty acid; HF rat, high-fat-fed rat; LCACoA, long-chain acyl-CoA.

© 2004 by the American Diabetes Association.

energy content was as follows: 59% fat, 20% carbohydrate, and 21% protein, with equal quantities of fiber, vitamins, and minerals as in the rat maintenance diet (11). One week before the study, the right jugular vein and left carotid artery were cannulated under general anesthesia (halothane). Catheters were exteriorized at the back of the neck to allow easy access. After the surgery, animals were handled daily to minimize stress, and only those that at least regained presurgery body weight were used for experiments.

The experiments were performed under conscious conditions in the postprandial period (3–5 h after food removal). After catheters were connected to blood sampling and tracer administration syringes, the rats were allowed to rest for 40–50 min. After basal (time 0) blood samples were taken, the animals were randomly assigned to receive a subcutaneous injection of either AICAR (250 mg/kg in saline; Sigma, St. Louis, MO) or an equivalent volume of normal saline as control. Blood samples were collected at 10, 20, 30, and 46 min. Plasma was separated by centrifugation to measure circulating concentrations of glucose, insulin, FAs, and lactate. Blood cells were resuspended in saline and returned to the animal. At 30 min, both control and AICAR-treated animals were divided into two groups. One group received a 4-min intravenous infusion of mixed FA tracers, consisting of  $^3\text{H}$ -R-BrP (supplied by AstraZeneca, Möndal, Sweden) and  $^{14}\text{C}$ -palmitate (purchased from Amersham Pharmaceutical Biosciences, Little Chalfont, U.K.). Arterial plasma samples (0.2 ml) were collected at 1, 2, 3, 4, 5, 6, 8, 12 and 16 min after the start of tracer administration, to determine the tracer disappearance rate (12). The other group of rats were administered with a bolus of mixed glucose tracers consisting of 2DG and  $^{14}\text{C}$ -glucose (Amersham Pharmaceutical Biosciences). For directly comparing both FA and glucose uptake at the same time, plasma samples were also collected at 1, 2, 3, 4, 5, 6, 8, 12, and 16 min after glucose tracer administration. After the last sample, rats were anesthetized with pentobarbital. Red and white quadriceps muscles were immediately removed, freeze clamped with aluminum tongs precooled in liquid nitrogen, and stored at  $-80^\circ\text{C}$  for subsequent analysis.

**Determination of plasma tracer concentration.** Plasma activities of  $^3\text{H}$ -R-BrP and  $^{14}\text{C}$ -palmitate were separated from total  $^3\text{H}$  and  $^{14}\text{C}$  at each time point, using an initial acid lipid extraction with a mixture of isopropanol-hexane–0.5 mol/l  $\text{H}_2\text{SO}_4$  (40:10:1) followed by a polarity separation step under alkaline conditions. This procedure partitions esterified FAs into a hexane phase and FAs in anionic form (including the  $^3\text{H}$ -R-BrP and  $^{14}\text{C}$ -P tracers) into an alcohol phase. Small corrections (<10%), based on separation of FAs and esterified FA standards, were used to correct for incomplete partitioning of tracer as described previously (12). For determining hexose tracer concentrations, plasma samples were deproteinized immediately in 2.75%  $\text{ZnSO}_4$  and saturated  $\text{Ba}(\text{OH})_2$ . An aliquot of the supernatant was used to determine  $^3\text{H}$  and  $^{14}\text{C}$  activities (13).

**Determination of tissue tracer content.** Tissue samples from rats that were administered FA tracers were homogenized in chloroform:methanol (2:1). An aliquot of the homogenate was taken to determine the total  $^3\text{H}$ -R-BrP activity, and the remaining tissue extract was spun at 3,500g for 15 min. The resultant supernatant was separated into aqueous and organic phases by the addition of 1 ml of distilled water and an additional 10-min spin at 3,500g. Tissue samples from rats that received an injection of hexose tracers were extracted to determine glucose uptake (from  $^3\text{H}$ -2DG) and glycogen synthesis (from  $^{14}\text{C}$ -glucose) by the method as previously published (14). Activities of  $^3\text{H}$  and  $^{14}\text{C}$  in appropriate plasma and tissue fractions were measured by a liquid-scintillation counter (Beckman Instruments, Fullerton, CA) using a dual-label protocol.

**Calculation of muscle glucose and FA uptake/storage.** A tissue clearance rate for each of the four tracers was calculated from the tissue content and plasma profile of radiolabeled substrate as previously described for glucose (13) and FAs (12). An index of the rate of substrate uptake was then calculated from the clearance estimate and circulating substrate concentration. For the nonmetabolizable tracers phospho- $^3\text{H}$ -2DG and  $^3\text{H}$ -R-BrP, total radiolabeled content in the tissue was used in the calculations. These tracers yielded indexes of total glucose uptake and total FA uptake, respectively. The metabolizable tracers  $^{14}\text{C}$ -glucose and  $^{14}\text{C}$ -palmitate were used to estimate the rate of glycogen synthesis and the rate of FA incorporation into lipid storage products (glyceride and phospholipids), respectively. For the glycogen synthesis calculations, only radiolabel specifically incorporated into glycogen was used (14). In the case of palmitate tracer, only the label found in the organic phase was used in calculations (15). From these results, the ratio of storage to total uptake was also calculated as an index on the intracellular partitioning of FAs.

The rates of FA uptake derived from the FA analog  $^3\text{H}$ -R-BrP are proportional to the uptake rates of circulating FA (12), but the constant of proportionality (lumped constant,  $\text{LC}^*$ ) is not unity. The results presented here have been corrected using previously determined values of  $\text{LC}^*$  (16). Similar considerations can apply to the glucose analog 2DG in some tissues.

However, no correction was applied here because the value for  $\text{LC}^*$  in muscle is close to 1 (13). The values of glucose uptake determined with the shorter protocol in the present study were compared with those determined with our usual 45-min protocol (13) in a separate experiment using  $^3\text{H}$ - and  $^{14}\text{C}$ -labeled 2DG. There was a highly significant correlation ( $r = 0.91$ ,  $P < 0.001$ ) between these two protocols across a wide range of tissues, including red and white muscles (data not shown).

**Biochemical measurements.** Plasma glucose and lactate were measured with a Yellow Springs glucose analyzer (YSI 2300, Yellow Springs, OH). Plasma FAs were determined spectrophotometrically with an acyl-CoA oxidase-based colorimetric kit (NEFA-C; WAKO Pure Chemical Industries, Osaka, Japan). Plasma insulin was measured by radioimmunoassay using a commercial kit (Linco, St. Louis, MO). AMPK activity in tissues was assayed in a buffer that contained 40 mmol/l HEPES (pH 7.0), 200  $\mu\text{mol/l}$  AMP, 200  $\mu\text{mol/l}$  ATP, 80 mmol/l NaCl, 8% glycerol, 0.8 mmol/l NaCl, 0.8 mmol/l dithiothreitol, and 200  $\mu\text{mol/l}$  [ $\gamma$ - $^{32}\text{P}$ ]ATP for 20 min at  $37^\circ\text{C}$  (17). The AMPK-specific AMARA peptide (18) (Auspep, Victoria, Australia) was used as a substrate. Muscle long-chain acyl-CoAs (LCACoAs) were extracted from 50 mg of tissue sample and determined by the method of Antinozzi et al. (19). Acyl-CoA synthetase activity in muscle was determined by measuring  $^{14}\text{C}$ -palmitate incorporation into palmitoyl-CoA as previously described (20). Tissue content of triglycerides and glycogen was measured as previously described (20,21). Tissue ZMP was extracted from 20 mg of tissue sample, and its accumulation was determined by high-performance liquid chromatography (HPLC). The method was identical to that of Ye et al. (22), except that the mobile phase had 10% acetonitrile instead of 5% and the column used for the separation was Atlantis dC18 3  $\mu\text{m}$ ,  $4.6 \times 150$  mm (Waters, Milford, MA).

**Statistical analysis.** Results are presented as mean  $\pm$  SE. One-way ANOVA followed by post hoc (Fisher's protected least significant difference) tests or a  $t$  test were used to assess statistical significance between groups.  $P \leq 0.05$  was regarded as statistically significant.

## RESULTS

Body weight (controls,  $390 \pm 4$ ; AICAR-treated,  $394 \pm 5$  g), plasma glucose, insulin, FAs, and lactate values were similar in rats that received either lipid or glucose tracers. Pooled data are shown in Fig. 1. AICAR injection caused an  $\sim 25\%$  decrease in plasma glucose from 20 min onward. This was accompanied by a progressive reduction in plasma insulin (by  $\sim 60\%$ ). AICAR also induced a transient decrease in plasma FAs (by  $\sim 30\%$ ) at 10 and 20 min, but this parameter returned to levels similar to the control group after 30 min. In the AICAR-treated group, there was a moderate elevation in plasma lactate, but only toward the end of the experiment.

Figure 2 shows the effect of AICAR on AMPK activity in muscle. At the dose of AICAR given (250 mg/kg, subcutaneously), there was no detectable difference in AMPK activity in red quadriceps muscle between control and AICAR-treated groups at the time when tissues were collected. In contrast, AICAR increased AMPK activity by  $\sim 80\%$  in white quadriceps muscle.

In the basal state, glucose uptake was approximately four times higher in red quadriceps compared with white quadriceps (Fig. 3). AICAR-induced changes in glucose and FA uptake into red and white quadriceps followed the patterns of altered AMPK activity. AICAR did not significantly affect glucose uptake in red quadriceps, whereas in white quadriceps, AICAR increased glucose uptake by fivefold, reaching a level equivalent to that in red quadriceps muscle of control rats. Similarly, in red quadriceps, there was no significant difference in FA uptake between control and AICAR-treated rats, whereas this parameter was increased by 2.4-fold in white quadriceps after AICAR treatment.

In red quadriceps, glycogen synthesis was not statistically different between control and AICAR-treated groups (Fig. 4). However, glycogen synthesis was increased by

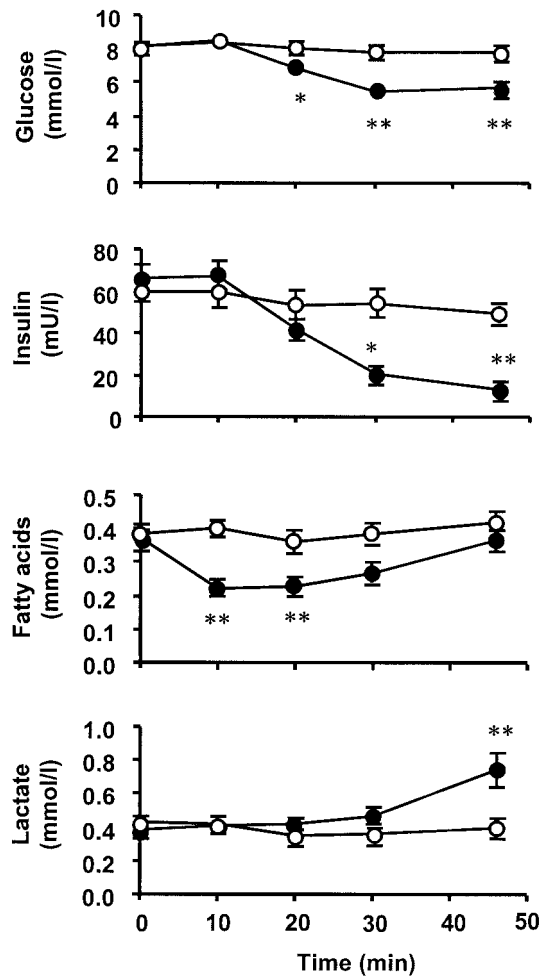


FIG. 1. Effects of AICAR on plasma levels of glucose, insulin, FAs, and lactate. AICAR (●) was injected subcutaneously immediately after the blood sample taken at 0 min, with normal saline used as control (○). Data from two sets of experiments were pooled together ( $n = 14$ /group). \* $P < 0.05$ , \*\* $P < 0.01$  vs. control.

sixfold in white quadriceps after AICAR treatment. Nevertheless, there was no detectable difference in glycogen mass in either red or white muscle after AICAR, compared with respective controls. There was a small increase in FA storage in red quadriceps as indicated by  $^{14}\text{C}$ -palmitate content and FA storage-to-uptake ratio (Table 1), indicating preferential partitioning of FAs toward storage. In white quadriceps, FA storage from  $^{14}\text{C}$ -palmitate was not significantly altered in AICAR-treated rats, but there was a

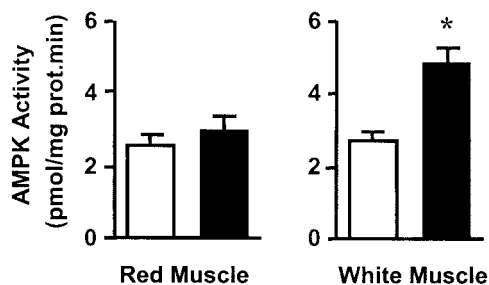


FIG. 2. Effects of AICAR on AMPK activity in red and white muscles. The enzyme activity was determined from muscle samples that were freeze clamped 46 min after AICAR administration (■). \*\* $P < 0.01$  vs. control (□;  $n = 6$ /group).

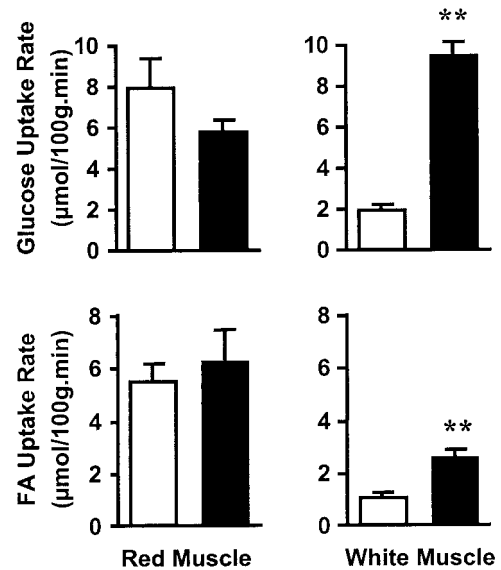


FIG. 3. Effects of AICAR on glucose and FA uptake in red and white muscles. Glucose uptake was determined using  $^3\text{H}$ -2DG content and the area of the plasma disappearance curve for this tracer. FA uptake was determined by  $^3\text{H}$ -R-BrP against the area of plasma disappearance curve of this tracer. ■, AICAR-treated group. \*\* $P < 0.01$  vs. control (□;  $n \geq 6$ /group).

40% decrease in FA storage-to-uptake ratio (Table 1), indicating increased catabolism of FAs. Although triglyceride content was only slightly decreased in red quadriceps by AICAR, LCACoA content was increased in both red (by 52%) and white (by 76%) muscles in AICAR-treated rats.

Because LCACoA content was increased in both red and white quadriceps, we measured the activity of acyl-CoA synthetase (ACS), a key enzyme that catalyzes the forma-

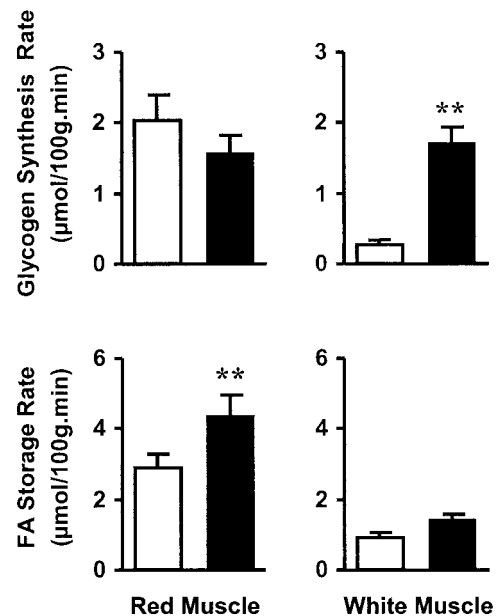


FIG. 4. Effects of AICAR on glycogen synthesis and FA storage in red and white muscles. Glycogen synthesis was determined by measuring  $^{14}\text{C}$ -glucose incorporation into glycogen against the area of plasma disappearance curve of this tracer. FA storage was determined by measuring  $^{14}\text{C}$ -palmitate content in the extracted lipid pool against the area of the plasma disappearance curve for this tracer. ■, AICAR-treated group. \*\* $P < 0.01$  vs. control (□;  $n \geq 6$ /group).

TABLE 1  
Effects of AICAR on lipid metabolites, ACS activity, and glycogen content in red and white muscles

	Red quadriceps		White quadriceps	
	Control	AICAR	Control	AICAR
FA storage/uptake ratio	0.48 ± 0.04	0.77 ± 0.14*	0.93 ± 0.10	0.55 ± 0.04**
Triglyceride content (μmol/g)	3.3 ± 0.4	2.4 ± 0.4**	4.0 ± 0.7	6.1 ± 1.1
LCACoA content (nmol/g)	20 ± 2	33 ± 3*	3.8 ± 0.3	6.8 ± 0.8**
ACS activity (pmol · mg <sup>-1</sup> · min <sup>-1</sup> )	142 ± 12	137 ± 8	28 ± 2	30 ± 3
Glycogen content (μmol/g)	43.5 ± 1.1	40.8 ± 1.3	27.7 ± 1.8	27.1 ± 1.8

Data are means ± SE. \**P* < 0.05, \*\**P* < 0.01 vs. control (*n* ≥ 6/group).

tion of LCACoAs from FAs. Consistent with the higher content of LCACoAs, ACS activity was five times higher in red quadriceps than in white quadriceps (*P* < 0.01). However, neither red nor white quadriceps of the AICAR-treated group showed any significant difference in ACS activity compared with the control group (Table 1).

In the AICAR-treated rats, ZMP levels were 0.135 ± 0.008 μmol/g in red quadriceps and 0.062 ± 0.008 μmol/g in white quadriceps. ZMP was not detected in muscles from the HF control group.

## DISCUSSION

The present study is the first demonstration that administration of AICAR to insulin-resistant HF rats simultaneously increases glucose and FA uptake into skeletal muscle in close association with activation of AMPK. These effects occurred preferentially in white muscle and were consistent with the previously described improvement of insulin sensitivity in white muscle 24 h after AICAR treatment (8). Contrary to our initial speculation, there was no higher FA uptake in red muscle to balance the lack of AICAR effect on glucose uptake in this muscle type.

It is known that fluxes of glucose and FA into muscle are increased from the circulation during exercise (1,23,24). Recent studies have revealed an important role of AMPK in exercise-induced changes in fuel metabolism (1,2). However, many other factors are also important metabolic regulators in contracting muscle (7), such as decreased energy storage (ATP and creatine phosphate content) (25), increases in metabolic rate, muscle blood flow, and plasma levels of catecholamines and interleukin-6 (26). Because AICAR activates AMPK without altering cell energy status (6,27) and AICAR-stimulated effects are independent of catecholamines (Iglesias et al., unpublished observations), our findings demonstrate that activation of AMPK is able to mediate profound simultaneous increases in glucose and FA uptake in white muscle. It is interesting that these effects occurred even though plasma insulin levels were substantially decreased, supporting the view that insulin is not a mediator for these changes (27).

It is of interest that activation of AMPK with AICAR in resting white quadriceps muscle of HF rats increases its FA uptake concomitantly with a substantial increase in glucose uptake, both fuel fluxes occurring in the absence of an increased energy demand, such as would occur during exercise. That both glucose and FA uptake were simultaneously increased by AICAR suggests that AMPK-mediated glucose and lipid metabolism in muscle are regulated beyond any substrate competition effects such

as the Randle cycle (28). It is now clear that activation of the AMPK pathway in muscle with AICAR increases glucose uptake via GLUT4 translocation (5,29), and this mechanism is at least partially responsible for the uptake of glucose during muscle contraction (7,29). Although activation of AMPK with AICAR may have direct effects on glycogen synthase and phosphorylase to inhibit glycogen synthesis (9), the substantial increase in glucose uptake without a demand for an increase in glucose oxidation may have overcome these effects, enhancing its storage by increasing glycogen synthesis (30).

During muscle contraction (31) or AICAR stimulation (6), activated AMPK mediates a reduction in malonyl-CoA via acetyl-CoA carboxylase and malonyl-CoA decarboxylase. Reduced malonyl-CoA in turn diminishes the inhibition of carnitine palmitoyltransferase-1 by malonyl-CoA and enhances the entry of LCACoAs into mitochondria for oxidation. This mechanism may underlie the increased FA catabolism in white muscle (as indicated by a decrease in FA storage-to-uptake ratio) in the present study. However, this mechanism alone would be predicted likely to result in a decrease in muscle LCACoA content. In the present study, white muscle LCACoA content was increased, suggesting that the metabolic pathway upstream of LCACoA formation may also be involved in AICAR stimulation of FA uptake. In an attempt to investigate this possibility, we examined the activity of ACS, the enzyme that catalyzes LCACoA synthesis. As the activity of this enzyme was not altered, ACS is probably not involved in AMPK-mediated FA uptake. A recent study showed that during muscle contraction, the increase in FA uptake in myocytes is associated with translocation of the FA transporter FAT/CD36 from the cytosol to the plasma membrane (32). It is possible that it also may be involved in increases in FA uptake and LCACoA content in muscle when AMPK is activated by AICAR, but further studies are required to investigate this possibility.

Another interesting finding in the present study is that AICAR increased AMPK activity preferentially in white muscle and that this was associated with substantially suppressed plasma glucose and FA levels. In the rat, 70% of muscle is composed of the IIb fiber type, the main component of white muscle (33). Therefore, the AMPK-mediated metabolic response in white skeletal muscle after AICAR administration would have an important influence on whole-body glucose and lipid homeostasis. This is consistent with our previous finding showing preferential enhancement of insulin action in white muscle and the whole body after AICAR administration (8).

The present study demonstrates that despite showing a

greater accumulation of ZMP, AMPK activity in red muscle is less sensitive to AICAR stimulation than in white muscle, as previously reported (34–36). The reason for this is not clear, but it seems to be a specific phenomenon in response to AICAR. AICAR and hypoxia have been shown to activate GLUT4 translocation by activation of  $\alpha$ -2 AMPK in muscle (7,37). It is possible that the greater oxidative capacity of red muscle is a factor in the lower sensitivity of AMPK to hypoxia or AICAR compared with white muscle. Alternatively, it might be related to a different level of expression of regulatory subunits of AMPK in white versus red muscle. For example, there is a fivefold greater expression of the  $\gamma$ -3 subunit in white muscle compared with red (38). Irrespective of the mechanisms for this difference, activation of AMPK has been shown to increase both glucose uptake and lipid oxidation in both red and white muscle after other stimuli such as exercise (39), leptin (40), and adiponectin (41). Nevertheless, although responses may be blunted, there seem to be some AMPK-related effects occurring in red muscle after AICAR. We found altered intramuscular lipid metabolism in red muscle, including increased LCACoA content, rate of FA storage, and decreased triglyceride content. It is not clear whether these changes are secondary to altered systemic lipids and thus not a direct tissue response to AICAR or are due to activation of AMPK at an earlier time point or to non-AMPK-related effects of AICAR (42). We cannot completely exclude nonspecific effects of AICAR, but that AICAR has no effect on muscle glucose transport in mutant mice with chronic inactivation of AMPK argues against significant nonspecific effects in muscle (43). It is probable that with a higher dose of AICAR, significant AMPK activation would be seen; in normal rats, glucose uptake was increased in red muscle along with significant AMPK activation when AICAR was administered intravenously at a dose approximately fourfold that injected subcutaneously in the present study (27). The factors that influence effects of AICAR on red muscle under different conditions need to be investigated further.

In summary, the present study shows that AICAR causes acute enhancement of both glucose and FA uptake in muscle of insulin-resistant HF rats in vivo. These effects principally occur in white rather than red muscle, consistent with the relative degree of activation of AMPK. Preferential acute effects of AICAR on metabolism in white muscle are also consistent with a subsequent preferential enhancement of insulin sensitivity in this type of muscle occurring beyond the duration of AMPK activation (8). Taking our two studies together, it seems that a greater enhancement of insulin sensitivity in white muscle after AICAR administration is related to mechanisms other than a lesser acute AMPK-induced increment in systemic FA uptake (and lesser tendency to accumulate cytosolic lipids). Other possible mechanisms will need to be investigated.

#### ACKNOWLEDGMENTS

Supported by grants from the National Health and Medical Research Council (Australia) and the Juvenile Diabetes Research Foundation (U.S.).

We thank Dr. Wenbo Qi, Mercedes Ballesteros, Joanna Edema, Lynn Croft, Donna Wilks, and the staff of the

Garvan's Biological Testing Facility for excellent technical assistance in this study.

#### REFERENCES

- Hayashi T, Hirshman MF, Kurth EJ, Winder WW, Goodyear LJ: Evidence for 5' AMP-activated protein kinase mediation of the effect of muscle contraction on glucose transport. *Diabetes* 47:1369–1373, 1998
- Vavvas D, Apazidis A, Saha AK, Gamble J, Patel A, Kemp BE, Witters LA, Ruderman NB: Contraction-induced changes in acetyl-CoA carboxylase and 5'-AMP-activated kinase in skeletal muscle. *J Biol Chem* 272:13255–13261, 1997
- Kemp BE, Mitchellhill KI, Stapleton D, Michell BJ, Chen ZP, Witters LA: Dealing with energy demand: the AMP-activated protein kinase. *Trends Biochem Sci* 24:22–25, 1999
- Saha AK, Schwarsin AJ, Roduit R, Masse F, Kaushik V, Tornheim K, Prentki M, Ruderman NB: Activation of malonyl-CoA decarboxylase in rat skeletal muscle by contraction and the AMP-activated protein kinase activator 5-aminoimidazole-4-carboxamide-1- $\beta$ -D-ribofuranoside. *J Biol Chem* 275:24279–24283, 2000
- Kurth-Kraczek EJ, Hirshman MF, Goodyear LJ, Winder WW: 5' AMP-activated protein kinase activation causes GLUT4 translocation in skeletal muscle. *Diabetes* 48:1667–1671, 1999
- Merrill GF, Kurth EJ, Hardie DG, Winder WW: AICA riboside increases AMP-activated protein kinase, fatty acid oxidation, and glucose uptake in rat muscle. *Am J Physiol* 273:E1107–E1112, 1997
- Mu J, Brozinick JT, Valladares O, Bucan M, Birnbaum MJ: A role for amp-activated protein kinase in contraction- and hypoxia-regulated glucose transport in skeletal muscle. *Mol Cell* 7:1085–1094, 2001
- Iglesias MA, Ye JM, Frangioudakis G, Saha AK, Tomas E, Ruderman NB, Cooney GJ, Kraegen EW: AICAR administration causes an apparent enhancement of muscle and liver insulin action in insulin-resistant high-fat-fed rats. *Diabetes* 51:2886–2894, 2002
- Wojtaszewski JF, Jorgensen SB, Hellsten Y, Hardie DG, Richter EA: Glycogen-dependent effects of 5-aminoimidazole-4-carboxamide (AICA)-riboside on AMP-activated protein kinase and glycogen synthase activities in rat skeletal muscle. *Diabetes* 51:284–292, 2002
- Kraegen EW, Cooney GJ, Ye JM, Thompson AL, Furler SM: The role of lipids in the pathogenesis of muscle insulin resistance and beta cell failure in type II diabetes and obesity. *Exp Clin Endocrinol Diabetes* 109:S189–S201, 2001
- Kraegen EW, James DE, Bennett SP, Chisholm DJ: In vivo insulin sensitivity in the rat determined by euglycemic clamp. *Am J Physiol* 245:E1–E7, 1983
- Oakes ND, Kjellstedt A, Forsberg GB, Clementz T, Camejo G, Furler SM, Kraegen EW, Olwegard-Halvarsson M, Jenkins AB, Ljung B: Development and initial evaluation of a novel method for assessing tissue-specific plasma free fatty acid utilization in vivo using (R)-2-bromopalmitate tracer. *J Lipid Res* 40:1155–1169, 1999
- Kraegen EW, James DE, Jenkins AB, Chisholm DJ: Dose-response curves for in vivo insulin sensitivity in individual tissues in rats. *Am J Physiol* 248:E353–E362, 1985
- James DE, Kraegen EW, Chisholm DJ: Effects of exercise training on in vivo insulin action in individual tissues of the rat. *J Clin Invest* 76:657–666, 1985
- Hegarty BD, Cooney GJ, Kraegen EW, Furler SM: Increased efficiency of fatty acid uptake contributes to lipid accumulation in skeletal muscle of high fat-fed insulin-resistant rats. *Diabetes* 51:1477–1484, 2002
- Furler SM, Cooney GJ, Hegarty BD, Lim-Fraser MY, Kraegen EW, Oakes ND: Local factors modulate tissue-specific NEFA utilization: assessment in rats using 3H-(R)-2-bromopalmitate. *Diabetes* 49:1427–1433, 2000
- Davies SP, Carling D, Hardie DG: Tissue distribution of the AMP-activated protein kinase, and lack of activation by cyclic-AMP-dependent protein kinase, studied using a specific and sensitive peptide assay. *Eur J Biochem* 186:123–128, 1989
- Dale S, Wilson WA, Edelman AM, Hardie DG: Similar substrate recognition motifs for mammalian AMP-activated protein kinase, higher plant HMG-CoA reductase kinase-A, yeast SNF1, and mammalian calmodulin-dependent protein kinase I. *FEBS Lett* 361:191–195, 1995
- Antinozzi PA, Segall L, Prentki M, McGarry JD, Newgard CB: Molecular or pharmacologic perturbation of the link between glucose and lipid metabolism is without effect on glucose-stimulated insulin secretion: a re-evaluation of the long-chain acyl-CoA hypothesis. *J Biol Chem* 273:16146–16154, 1998
- Ellis BA, Poynten A, Lowy AJ, Furler SM, Chisholm DJ, Kraegen EW, Cooney GJ: Long-chain acyl-CoA esters as indicators of lipid metabolism

- and insulin sensitivity in rat and human muscle. *Am J Physiol* 279:E554–E560, 2000
21. Chan TM, Exton JH: A rapid method for the determination of glycogen content and radioactivity in small quantities of tissue or isolated hepatocytes. *Anal Biochem* 71:96–105, 1976
  22. Ye J, Clark MG, Colquhoun EQ: Creatine phosphate as the preferred early indicator of ischemia in muscular tissues. *J Surg Res* 61:227–236, 1996
  23. Ponticos M, Lu QL, Morgan JE, Hardie DG, Partridge TA, Carling D: Dual regulation of the AMP-activated protein kinase provides a novel mechanism for the control of creatine kinase in skeletal muscle. *EMBO J* 17:1688–1699, 1998
  24. Holloszy JO, Kohrt WM, Hansen PA: The regulation of carbohydrate and fat metabolism during and after exercise. *Front Biosci* 3:D1011–D1027, 1998
  25. Hardie DG, Carling D: The AMP-activated protein kinase—fuel gauge of the mammalian cell? *Eur J Biochem* 246:259–273, 1997
  26. Helge JW, Stallknecht B, Pedersen BK, Galbo H, Kiens B, Richter EA: The effect of graded exercise on IL-6 release and glucose uptake in human skeletal muscle. *J Physiol* 546:299–305, 2003
  27. Bergeron R, Russell RR 3rd, Young LH, Ren JM, Marcucci M, Lee A, Shulman GI: Effect of AMPK activation on muscle glucose metabolism in conscious rats. *Am J Physiol* 276:E938–E944, 1999
  28. Randle PJ, Hales CN, Garland PB, Newsholme EA: The glucose fatty-acid cycle. Its role in insulin sensitivity and the metabolic disturbances of diabetes mellitus. *Lancet* 1:785–789, 1963
  29. Lemieux K, Konrad D, Klip A, Marette A: The AMP-activated protein kinase activator AICAR does not induce GLUT4 translocation to transverse tubules but stimulates glucose uptake and p38 mitogen-activated protein kinases  $\alpha$  and  $\beta$  in skeletal muscle. *FASEB J* 17:1658–1665, 2003
  30. Aschenbach WG, Hirshman MF, Fujii N, Sakamoto K, Howlett KF, Goodyear LJ: Effect of AICAR treatment on glycogen metabolism in skeletal muscle. *Diabetes* 51:567–573, 2002
  31. Park H, Kaushik VK, Constant S, Prentki M, Przybytkowski E, Ruderman NB, Saha AK: Coordinate regulation of malonyl-CoA decarboxylase, sn-glycerol-3-phosphate acyltransferase, and acetyl-CoA carboxylase by AMP-activated protein kinase in rat tissues in response to exercise. *J Biol Chem* 277:32571–32577, 2002
  32. Bonen A, Luiken JJ, Arumugam Y, Glatz JF, Tandon NN: Acute regulation of fatty acid uptake involves the cellular redistribution of fatty acid translocase. *J Biol Chem* 275:14501–14508, 2000
  33. Delp MD, Duan C: Composition and size of type I, IIA, IID/X, and IIB fibers and citrate synthase activity of rat muscle. *J Appl Physiol* 80:261–270, 1996
  34. Ai H, Ihlemann J, Hellsten Y, Lauritzen HP, Hardie DG, Galbo H, Ploug T: Effect of fiber type and nutritional state on AICAR- and contraction-stimulated glucose transport in rat muscle. *Am J Physiol Endocrinol Metab* 282:E1291–1300, 2002
  35. Jessen N, Pold R, Buhl ES, Jensen LS, Schmitz O, Lund S: Effects of AICAR and exercise on insulin-stimulated glucose uptake, insulin signaling and GLUT4 content in rat skeletal muscles. *J Appl Physiol* 94:1373–1379, 2003
  36. Stoppani J, Hildebrandt AL, Sakamoto K, Cameron-Smith D, Goodyear LJ, Neuffer PD: AMP-activated protein kinase activates transcription of the UCP3 and HKII genes in rat skeletal muscle. *Am J Physiol Endocrinol Metab* 283:E1239–E1248, 2002
  37. Jorgensen SB, Viollet B, Andreelli F, Frogis C, Birk JB, Schjerling P, Vaultont S, Richter EA, Wojtaszewski JF: Knockout of the  $\alpha 2$  but not  $\alpha 1$  5'-AMP-activated protein kinase isoform abolishes 5-aminoimidazole-4-carboxamide-1- $\beta$ -D-ribofuranoside but not contraction-induced glucose uptake in skeletal muscle. *J Biol Chem* 279:1070–1079, 2004
  38. Mahlapuu M, Johansson C, Lindgren K, Hjalml G, Barnes BR, Krook A, Zierath JR, Andersson L, Marklund S: Expression profiling of the  $\gamma$ -subunit isoforms of AMP-activated protein kinase suggests a major role for  $\gamma 3$  in white skeletal muscle. *Am J Physiol Endocrinol Metab* 286:E194–E200, 2004
  39. Rasmussen BB, Winder WW: Effect of exercise intensity on skeletal muscle malonyl-CoA and acetyl-CoA carboxylase. *J Appl Physiol* 83:1104–1109, 1997
  40. Minokoshi Y, Kim YB, Peroni OD, Fryer LG, Muller C, Carling D, Kahn BB: Leptin stimulates fatty-acid oxidation by activating AMP-activated protein kinase. *Nature* 415:339–343, 2002
  41. Yamauchi T, Kamon J, Minokoshi Y, Ito Y, Waki H, Uchida S, Yamashita S, Noda M, Kita S, Ueki K, Eto K, Akanuma Y, Froguel P, Foufelle F, Ferre P, Carling D, Kimura S, Nagai R, Kahn BB, Kadowaki T: Adiponectin stimulates glucose utilization and fatty-acid oxidation by activating AMP-activated protein kinase. *Nat Med* 7:7, 2002
  42. Lefebvre DL, Bai Y, Shahmolky N, Sharma M, Poon R, Drucker DJ, Rosen CF: Identification and characterization of a novel sucrose-non-fermenting protein kinase/AMP-activated protein kinase-related protein kinase, SNARK. *Biochem J* 355:297–305, 2001
  43. Viollet B, Andreelli F, Jorgensen SB, Perrin C, Geloan A, Flamez D, Mu J, Lenzner C, Baud O, Bennoun M, Gomas E, Nicolas G, Wojtaszewski JF, Kahn A, Carling D, Schuit FC, Birnbaum MJ, Richter EA, Burcelin R, Vaultont S: The AMP-activated protein kinase  $\alpha 2$  catalytic subunit controls whole-body insulin sensitivity. *J Clin Invest* 111:91–98, 2003